

ARMY RESEARCH LABORATORY



Characterization of Attocube Nanopositioners for Vibration

by Dimitri Alexson and Doran D. Smith

ARL-TR-5315

September 2010

NOTICES

Disclaimers

The findings in this report are not to be construed as an official Department of the Army position unless so designated by other authorized documents.

Citation of manufacturer's or trade names does not constitute an official endorsement or approval of the use thereof.

Destroy this report when it is no longer needed. Do not return it to the originator.

Army Research Laboratory

Adelphi, MD 20783-1197

ARL-TR-5315

September 2010

Characterization of Attocube Nanopositioners for Vibration

Dimitri Alexson and Doran D. Smith
Sensors and Electron Devices Directorate, ARL

REPORT DOCUMENTATION PAGE

Form Approved
OMB No. 0704-0188

Public reporting burden for this collection of information is estimated to average 1 hour per response, including the time for reviewing instructions, searching existing data sources, gathering and maintaining the data needed, and completing and reviewing the collection information. Send comments regarding this burden estimate or any other aspect of this collection of information, including suggestions for reducing the burden, to Department of Defense, Washington Headquarters Services, Directorate for Information Operations and Reports (0704-0188), 1215 Jefferson Davis Highway, Suite 1204, Arlington, VA 22202-4302. Respondents should be aware that notwithstanding any other provision of law, no person shall be subject to any penalty for failing to comply with a collection of information if it does not display a currently valid OMB control number.

PLEASE DO NOT RETURN YOUR FORM TO THE ABOVE ADDRESS.

1. REPORT DATE (DD-MM-YYYY) September 2010		2. REPORT TYPE Final		3. DATES COVERED (From - To) August 2010	
4. TITLE AND SUBTITLE Characterization of Attocube Nanopositioners for Vibration				5a. CONTRACT NUMBER	
				5b. GRANT NUMBER	
				5c. PROGRAM ELEMENT NUMBER	
6. AUTHOR(S) Dimitri A. Alexson and Doran D. Smith				5d. PROJECT NUMBER	
				5e. TASK NUMBER	
				5f. WORK UNIT NUMBER	
7. PERFORMING ORGANIZATION NAME(S) AND ADDRESS(ES) U.S. Army Research Laboratory ATTN: RDRL-SEE-O 2800 Powder Mill Road Adelphi, MD 20783-1197				8. PERFORMING ORGANIZATION REPORT NUMBER ARL-TR-5315	
9. SPONSORING/MONITORING AGENCY NAME(S) AND ADDRESS(ES)				10. SPONSOR/MONITOR'S ACRONYM(S)	
				11. SPONSOR/MONITOR'S REPORT NUMBER(S)	
12. DISTRIBUTION/AVAILABILITY STATEMENT Approved for public release; distribution unlimited.					
13. SUPPLEMENTARY NOTES					
14. ABSTRACT This report describes a series of vibration tests performed on nanopositioners manufactured by the company Attocube. Our goal was to determine if a cantilever mounted in a holder on top of an XYZ nanopositioner vibrated more than the Brownian motion of the cantilever at 4 K. We know that when the cantilever is mounted on a solid mechanical base that it does not vibrate more than the appropriate Brownian motion. The concern about the Attocube nanopositioner is that since it possesses mechanical resonances in the 1-kHz area, it might vibrate too much and, hence, excite the cantilever. We find that the Brownian motion of the cantilever mounted on the XYZ nanopositioner is what it should be for the temperature; however, the frequency noise is greater than the Brownian motion would predict. At this time, this result is not understood.					
15. SUBJECT TERMS Vibration, nanopositioner, attocube, cantilever, thermal					
16. SECURITY CLASSIFICATION OF:			17. LIMITATION OF ABSTRACT UU	18. NUMBER OF PAGES 22	19a. NAME OF RESPONSIBLE PERSON Doran D. Smith
a. REPORT Unclassified	b. ABSTRACT Unclassified	c. THIS PAGE Unclassified			19b. TELEPHONE NUMBER (Include area code) (301) 394-1918

Contents

List of Figures	iv
1. Introduction	1
2. Methods, Assumptions, and Procedures	3
3. Results and Discussion—Stiff Cantilever	8
4. Results and Discussion—Soft Cantilever	10
5. Conclusions	13
6. References	14
List of Symbols, Abbreviations, and Acronyms	15
Distribution List	16

List of Figures

Figure 1. Large amplitude IF calibration: four items are shown here: (1) raw data points are the red filled circles, (2) a straight line fit to the first three data points is the straight red line, (3) the sinusoidal fit to the data is green, and (4) the slope of the sinusoidal fit at zero is a green straight line.	5
Figure 2. Running standard deviation of cantilever motion; the standard deviation squared of $x(t)$ is equivalent to the measured value of $\langle x(t)^2 \rangle$	6
Figure 3. Running mean of cantilever motion; the two lines correspond to the running mean of the x and y components of the software lock-in output.	7
Figure 4. The puff ball; each chunk of data is plotted as a point at its corresponding x and y values.	7
Figure 5. Stiff cantilever $\langle x(t)^2 \rangle$ vs. temperature. The failure of the data to line on a straight line indicates the cantilever is being base driven. The straight line is a best fit to the data.	8
Figure 6. FT of 10 s of stiff cantilever $x(t)$. The Brownian motion peak occurs at 0 Hz and the baseline noise is due to IF shot noise.	9
Figure 7. Average FT of all stiff cantilever data collected. The area under the peak corresponds to $\langle x(t)^2 \rangle$ for the cantilever which sits on a noise baseline.	9
Figure 8. Soft cantilever $\langle x(t)^2 \rangle$ vs. temperature. Since the data all fall on a straight line down to the lowest temperature investigated, we know it is not significantly base driven and all of $\langle x(t)^2 \rangle$ can be attributed to Brownian motion. The straight line is a fit to the data and gives a spring constant of 0.000103 N/m.	10
Figure 9. Soft cantilever frequency noise vs. temperature. Data plotted as squares is for a cantilever driven close loop. The circles are the undriven cantilever measured during ring down.	12

1. Introduction

The nano-magnetic resonance imaging (MRI) laboratory of the U.S. Army Research Laboratory (ARL) performs mechanically detected magnetic resonance at cryogenic temperatures, typically 5 K. The system used to do this consists of a cryogenic probe immersed in liquid helium (He) and room-temperature electronic instrumentation. The major components of the probe consist of a vacuum jacket surrounding a probe head. The probe head has four components: (1) a radio frequency (RF) coil, (2) a cantilever with a tiny ferromagnet mounted on it, (3) an optical fiber, and (4) a sample mounted on a sample stage. The RF coil generates the RF magnetic field used to excite magnetic resonance in the sample. Magnetic resonance in the sample then excites the cantilever by interacting with the ferromagnet mounted on it. The motion of the cantilever is detected by the optical fiber.

Historically, we have always mounted the sample on a three-dimensional (3-D) nanopositioner and the cantilever is mounted on a more rigid mechanical base. However, collaborators at Cornell University plan to build a probe that requires the cantilever to be mounted on the nanopositioner and the sample on the more rigid mechanical base. Since, at this time, they do not have a probe with sufficient flexibility to allow them to mount the cantilever on the nanopositioner and we do, ARL is making vibration measurements for Cornell.

The 3-D nanopositioner used in our probe head is the XYZ 101 series nanopositioner by Attocube. Specifically, the nanopositioner is composed of a stack of three individual elements: one moving in the z direction, the ANPz101; one moving in the y direction, ANPx101; and one moving in the x direction, ANPx101. On the top of the 3-D nanopositioner is a sample stage. ARL designed a new sample stage to hold a cantilever instead of a sample. Cornell machined the new sample stage and we installed it in place of our sample stage. Without any further modification of our probe head, we were able to use our optical fiber to measure the motion of the cantilever mounted on top of the 3-D nanopositioner stack.

Two approaches were used to measure the Brownian motion of the cantilever. For the first, the instantaneous position of the undriven cantilever versus time was recorded. From this, the root mean square (RMS) value of its position was calculated. The RMS value of the cantilever position should equal the cantilever's Brownian motion for its base temperature. The second technique involved measuring the frequency noise of a driven cantilever. Hammel (1) and Marohn (2) have derived a theory that relates the driven cantilever's frequency noise to the Brownian motion. Experimental results of the Marohn group has shown that in some situations driven cantilevers have more frequency noise than is predicted by their Brownian motion alone (3).

The Brownian motion of a cantilever can be very simply predicted using the equal partition theorem. The equal partition theorem states that

$$k_c \langle x^2 \rangle = k_B T \quad (1)$$

where k_c is the cantilever spring constant, $\langle x^2 \rangle$ is the RMS value of the instantaneous position, k_B is Boltzmann's constant, and T is the absolute temperature. The temperature can be measured with an independent temperature sensor, k_B is a known constant, and $\langle x^2 \rangle$ is measured; therefore, the only unknown is k_c . The cantilever spring constant can be determined by measuring the RMS value of the cantilever motion at several different temperatures. If $\langle x^2 \rangle$ is plotted versus T , a straight line with a zero intercept should result. If the line bends toward the $\langle x^2 \rangle$ axis as T decreases, it means the cantilever is being base driven by vibrations. Base driving a cantilever means shaking the base of the cantilever, causing the tip to move, as opposed to moving the cantilever by applying forces directly to the tip of the cantilever. This approach serves as the basis for the first technique of measuring the Brownian motion of the cantilever. If the plot of $\langle x^2 \rangle$ versus T is a straight line, then a valid value for the Brownian motion of the cantilever has been obtained, unpolluted by vibrations.

The second technique for measuring Brownian motion involved measuring the frequency noise of a driven cantilever. A driven cantilever is a cantilever that is excited to a constant oscillation amplitude at its natural resonance frequency. We base drove the cantilever by exciting the X stage of the Attocube nanopositioner stack.

To determine the frequency and frequency noise of the cantilever, the position, x , of the cantilever is recorded versus time $x(t)$. Then $x(t)$ is extracted from the recorded data with a software lock-in implemented in LabVIEW*. The software lock-in is implemented by multiplying $x(t)$ against a sine wave, $\sin(2\pi f_0 t)$ and a cosine wave, $\cos(2\pi f_0 t)$, where the local oscillator f_0 is near the cantilever frequency f_c . The result of each product results in sum and difference terms:

$$\sin(2\pi f_c t) * \sin(2\pi f_0 t) = \frac{1}{2}(\cos(2\pi (f_0 - f_c) t) - \cos(2\pi (f_0 + f_c) t)) \quad (2)$$

$$\sin(2\pi f_c t) * \cos(2\pi f_0 t) = \frac{1}{2}(\sin(2\pi (f_0 - f_c) t) + \sin(2\pi (f_0 + f_c) t)) \quad (3)$$

The sum terms are each about $2f_c$ and the difference terms are slowly varying terms with a frequency of $(f_0 - f_c)$. A low pass digital filter is then used to filter the sum and difference terms. The $2f_c$ product is filtered out and only the difference terms are retained. The difference term resulting from the sine multiplication is called the X channel of the software lock-in; the cosine is the Y channel. For each $x(t)$ point we then calculate the arctangent of the ratio of the sine and cosine terms, resulting in a phase angle. This phase angle is the phase of the difference terms. We then unwrap the phase, i.e., each time the phase jumps from $+180^\circ$ to -180° , we add 360° to it so that a continuous line is formed. The unwrapped phase angle terms are then divided into

*LabVIEW is a trademark of National Instruments Corporation.

small segments termed “chunks” with about two chunks per f_c cycle. The slope of this line is determined for each chunk and the slope of the phase of a signal is its frequency. This results in a measure of the frequency of the difference terms versus time. Adding f_c to these terms provides a measurement of the original f_c versus time. From the f_c time record, we can perform any desired statistical analysis. For example, forming the power spectral density (PSD) of the frequency of the difference terms gives a PSD of the frequency deviations (frequency noise) of the cantilever around f_c .

The Marohn group has reported observing a cantilever with 4 K Brownian motion to have 77 K frequency noise (4). Therefore, in this work, we measured both and used those measurements to characterize how well the Attocube nanopositioners performed as a cantilever support.

2. Methods, Assumptions, and Procedures

To characterize the nanopositioners, we used an existing magnetic resonance force microscopy (MRFM) system custom built by ARL. The MRFM system consists of room-temperature electronics and a cryogenic probe (P5, for the fifth MRFM probe ARL has built) directly immersed in liquid He. The cryogenic part of the probe consists of a vacuum jacket surrounding a vibration-isolated probe head. A superconducting magnet can apply up to a 9 T magnetic field to the probe head. Since the magnetic field will create eddy current damping in the metallic body of the probe head when the probe vibrates, all experiments were preformed in a zero magnetic field to maximize the vibrations the nanopositioners experience.

The total mass of the probe head is approximately 0.5 kg. It is vibration isolated by suspension using three beryllium-copper (BeCu) springs. In the interior of each of the springs is inserted a Teflon[†] rod. When the probe head vibrates on the springs, the rubbing of the Teflon rods creates just enough friction to help damp out the vibrations. ARL has preformed experiments demonstrating that using the Teflon does decrease the amount of vibration the probe head experiences.

Probe head P5 was designed with the cantilever mounted on the probe head’s mechanical ground and the sample held by a sample stage mounted on a XYZ stack of Attocube nanopositioners. The regular sample stage was replaced with a custom cantilever holder designed by ARL and machined by Eric Moore of Cornell University. The cantilevers were held in such a position that the probe’s original optical fiber-based interferometer (IF) could be used to measure its position. Aligning the cantilever to the fiber by driving the nanopositioners in 3-D was very convenient. On the sample stage was mounted a silicon (Si) diode temperature sensor and a Nichrome wire heater with about 20 ohms resistance. By passing 100 mA at 2.0 V through the heater, it was

[†]Teflon is a registered trademark of E.I. DuPont de Nemours & Co., Inc.

possible to heat the sample stage to 40 K. The cantilever holder was thermally connected to the probe head's mechanical ground via a strip of Cu foil clamped between the bottom of the cantilever holder and the top of the nanopositioners. The Cu foil is used to thermally ground the cantilever holder since the thermal resistance and thermal time constant of the nanopositioner stack is unknown and measuring it was beyond the scope of this study. Later it may be determined to be unnecessary.

The probe head was then thermally connected to the probe vacuum jacket via three strips of Cu foil. These Cu foils are in parallel with the springs and couple in unwanted vibrations. The competing requirements of vibration isolation and removal of the heat generated by the RF must be balanced. The Cu foils were each 99.9999% pure, 25 μm thick, 1 cm wide, and 10 cm long between their clamped ends (7). We typically only use one Cu foil in parallel with the springs, but in this test we elected to use three to couple more vibrations into the probe head. One foil would not be enough to conduct out the 0.2 to 1.0 W Cornell wants dissipated from their probe head without unduly heating the probe head. A single annealed foil of the above dimensions has a measured by us to yield a temperature rise of 4.0 K for 200 mW with the cold end near 5 K.

Two cantilevers were used to characterize the nanopositioners. The stiff cantilever was made of silicon nitride (SiN) (5) with a spring constant of 0.01 N/m. It was mass loaded with a 75- μm glass sphere resulting in a cantilever resonant frequency of 1045 Hz. The soft cantilever was made of crystalline Si (6) with a spring constant of 0.0001 N/m, was not mass loaded, and had a resonant frequency 2398 Hz. The stiff cantilever is more sensitive to vibrations for two reasons: (1) the stiffer a cantilever is, the easier it is to base drive; and (2) typically there are more environmental vibrations coupled into the probe head at lower frequencies, with a significant falloff above 3 kHz.

To determine if the cantilever motion observed at 4 K was all Brownian motion or part base driving from probe head vibrations, we measured the Brownian motion as a function of temperature. The majority of thermal expansion of most material has occurred by the time it reaches the 4–20 K temperature range; however, not completely. As we vary the temperature from 5 to 20 K, it is necessary to retune the IF. The IF is tuned by varying the temperature of the IF's laser diode (8), which changes its wavelength. This procedure is repeated at each temperature since the determination of the amplitude of the Brownian motion is dependent upon accurate calibration of the IF sensitivity.

ARL determines the IF sensitivity by a calibration process called "Large Amplitude IF Calibration." The calibration process involves base driving the cantilever from amplitudes small with respect to a fringe length, one half of the IF wavelength, to an amplitude larger than one fringe length in even steps. If the IF behaves ideally, the interference fringe should have a sinusoidal shape as the IF wavelength is varied or as the cantilever is driven to larger amplitudes. This means for small amplitudes (the amplitudes relevant for measuring Brownian motion) the response is indistinguishable from linear, but as the amplitude becomes a sizable fraction of a

fringe length the IF response begins to roll over, as seen in figure 1. We fitted a few points in the linear region to a straight line to obtain the IF sensitivity. We also fitted the entire amplitude response to a sine wave. We compared the slope of the fitted sine wave to the linear fit near zero. They should agree. This serves two purposes. First, it provides a check to determine if the mathematics used to derive IF sensitivity near zero was performed correctly. Secondly, it determines how much distortion is in the IF sensitivity. We find the fringe shape is frequently close to sinusoidal, but not always. We believe that sometimes there are multiple optical paths interfering, possibly due to features on the cantilever's surface.

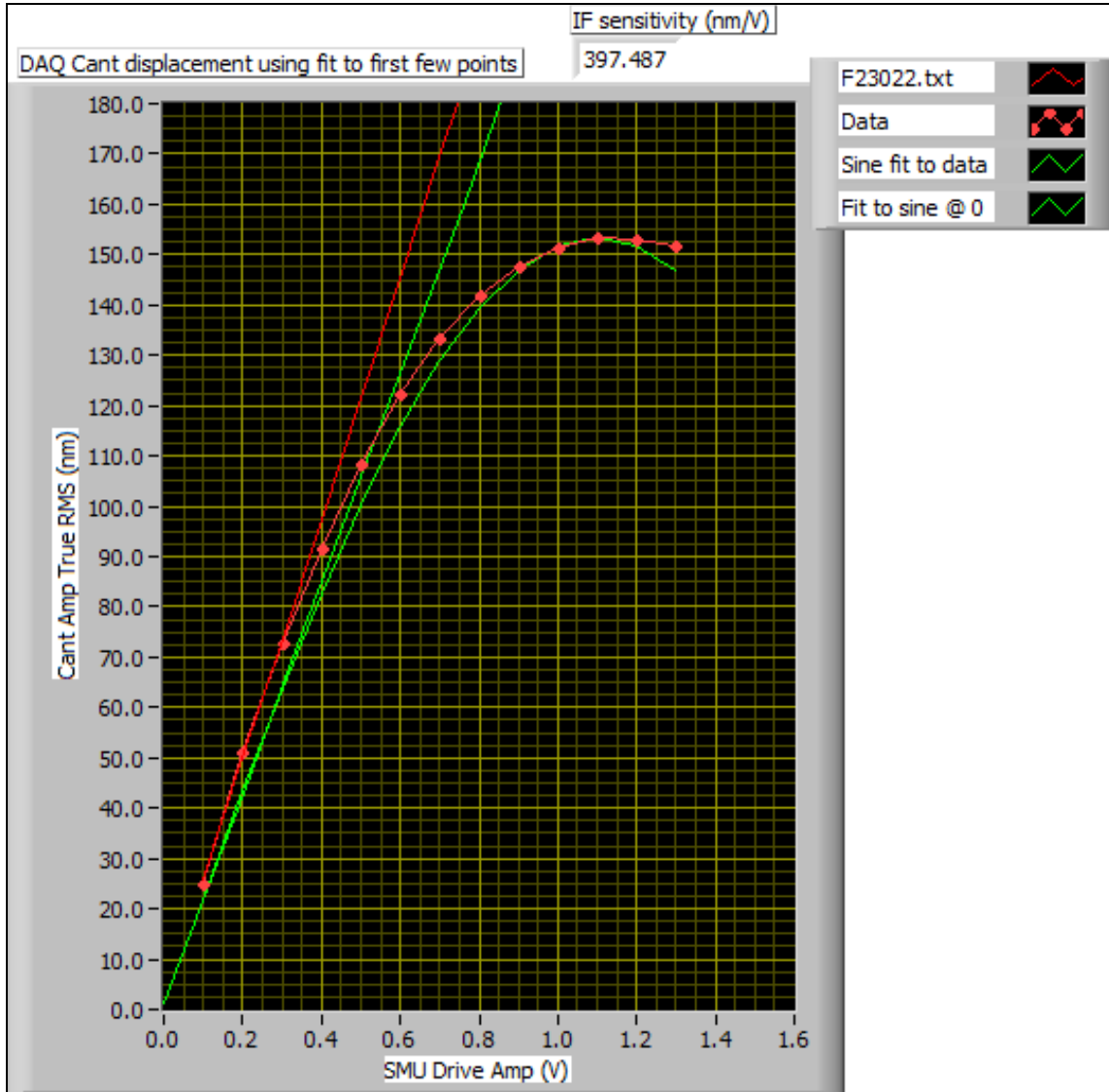


Figure 1. Large amplitude IF calibration: four items are shown here: (1) raw data points are the red filled circles, (2) a straight line fit to the first three data points is the straight red line, (3) the sinusoidal fit to the data is green, and (4) the slope of the sinusoidal fit at zero is a green straight line.

To determine an accurate value of the Brownian motion of the cantilever, we must determine the average value of $\langle x(t)^2 \rangle$ accurately. Data collection must be long enough so that the measured value of $\langle x(t)^2 \rangle$ has converged to its actual value. We measure the Brownian motion of our cantilevers without feedback, so it is a long, slow process. Each independent measurement of $\langle x(t)^2 \rangle$ requires about three times the damping time of the cantilever. Therefore, for a high Q cantilever, 20 min of data collection time can be required. Theoretically, to get $\langle x(t)^2 \rangle$ to converge, it is the error in the mean that we must get to a sufficiently small value. However, in practice, we watch the time-dependent values of the standard deviation (figure 2) and mean of $x(t)$ (figure 3). When the standard deviation becomes flat and the means of both the in-phase and out-of-phase channels converge to zero, we assume that we have collected data for long enough. For well-behaved cantilevers, i.e., not base driven, this assumption has been shown to result in plots of $\langle x(t)^2 \rangle$ versus T that were straight lines through zero.

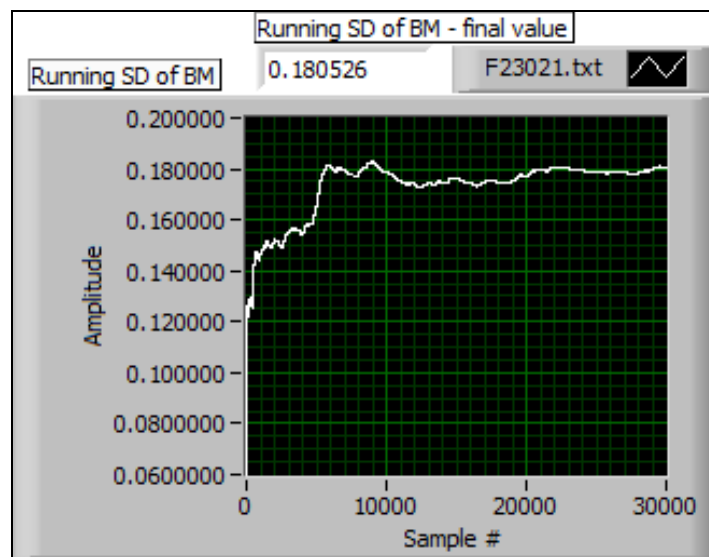


Figure 2. Running standard deviation of cantilever motion; the standard deviation squared of $x(t)$ is equivalent to the measured value of $\langle x(t)^2 \rangle$.

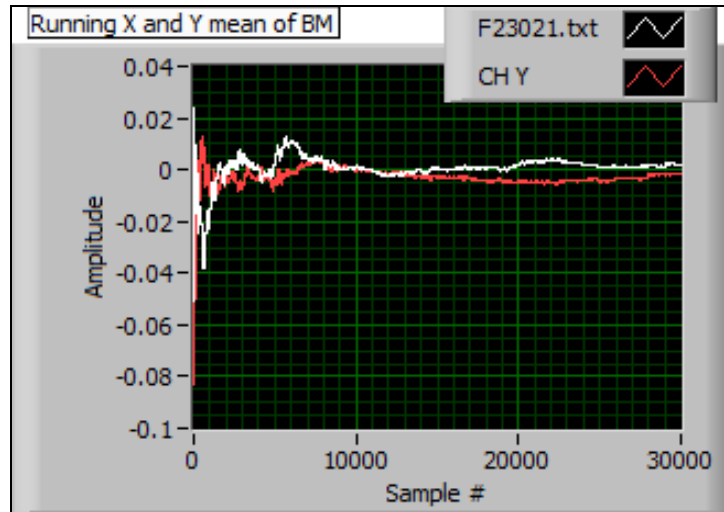


Figure 3. Running mean of cantilever motion; the two lines correspond to the running mean of the x and y components of the software lock-in output.

An additional check on the quality of the data is plotted in what is termed the “puff ball,” as shown in figure 4. Here, we plot every chunk of data as a point using its x and y values. For well-behaved data, the puff ball should be a well-formed round circle without too many outlying points. If that is not the case, something undesired has occurred during the data collection.

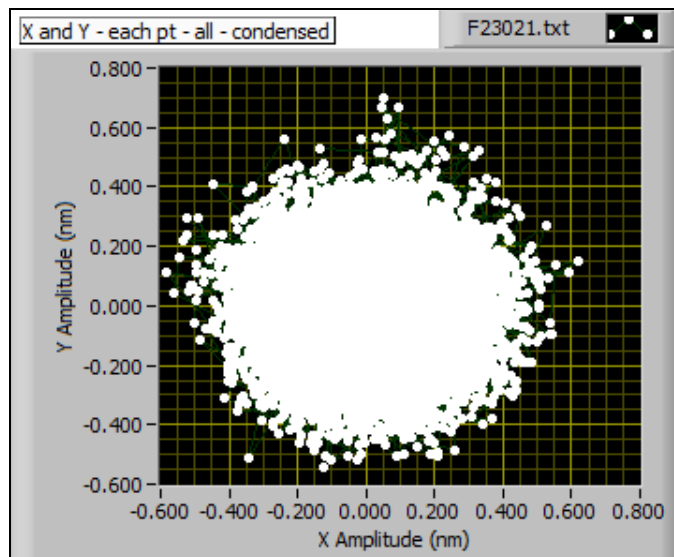


Figure 4. The puff ball; each chunk of data is plotted as a point at its corresponding x and y values.

For this work, data were collected using a 16 bit analog-to-digital converter (ADC) at 100 kilosamples per second for 12 s at a time. All 12 s of data underwent analysis as previously

described and then the first two seconds were discarded since it took a little less than 2 s for all the digital filters in the software lock-in to achieve steady-state. We determined that 60–80 data collection cycles were required to obtain a reasonable convergence of the data.

3. Results and Discussion—Stiff Cantilever

Figure 5 shows $\langle x(t)^2 \rangle$ versus temperature for the stiff cantilever. Clearly, it is not a straight line through zero. A data point taken at 77 K (not shown) had a $x(t)$ of 82 K, basically Brownian motion, while all the data from 5 to 22 K show the effect of vibrations. We conclude that the cantilever is base driven by vibrations, resulting in an effective temperature of about 30 K.

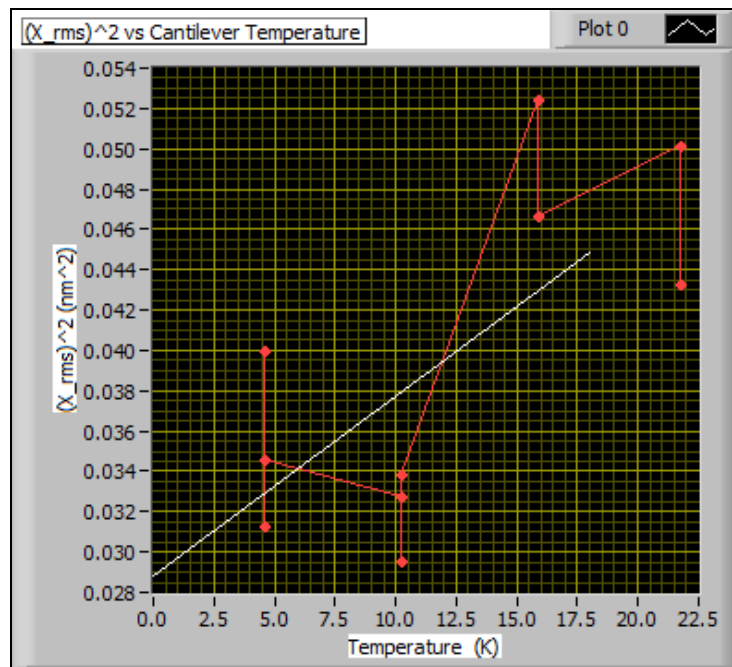


Figure 5. Stiff cantilever $\langle x(t)^2 \rangle$ vs. temperature. The failure of the data to line on a straight line indicates the cantilever is being base driven. The straight line is a best fit to the data.

This was the first time we used a stiff cantilever with the software lock-in. The amplitude of the Brownian motion of the stiff cantilever was 10 times less than that of the soft cantilevers we typically use. This resulted in $x(t)$ being close to the noise floor. For what we believe to be equivalent bandwidths, we found the Stanford Research Instruments SRS830 lock-in did a better job of filtering out the noise than our software lock-in did. Previously, the SRS830 was the only lock-in we had used on stiff cantilevers. Without more study, we cannot say what caused the difference. However, by adjusting the bandwidths, our software lock-in achieved the same signal-to-noise ratio (SNR) as the SRS830. We suspect the difference was due to different filter shapes, and hence, different effective bandwidths.

Because of this SNR problem, we performed one additional check on the data. We Fourier transformed (FT) the output of the software lock-in. The FT for one 10 s data set in the vicinity of the cantilever resonance is shown in figure 6. This figure contains two features: a noisy baseline and a peak due to $x(t)$. The average FT for 60 separate data collection cycles is shown in figure 7. The noisy baseline has converged and the $x(t)$ peak is well defined. By fitting a straight line to the noise baseline, we subtracted the noise off the FT peak. The area under the FT peak is known to be equal to $\langle x(t)^2 \rangle$ if the source of $x(t)$ is all Brownian motion (9). This should give us a better measure of the true value of $\langle x(t)^2 \rangle$ versus temperature. Performing the FT analysis on the data did not get it to lie on a straight line. Again, we conclude the cantilever is being base driven by environmental vibrations.

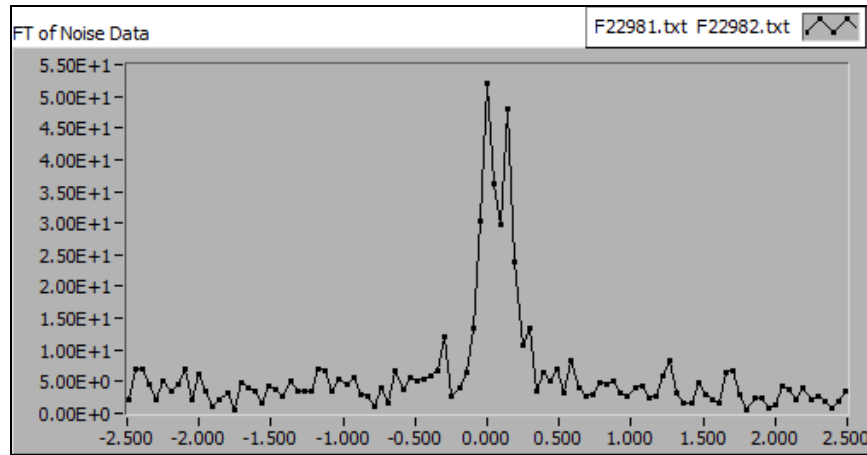


Figure 6. FT of 10 s of stiff cantilever $x(t)$. The Brownian motion peak occurs at 0 Hz and the baseline noise is due to IF shot noise.

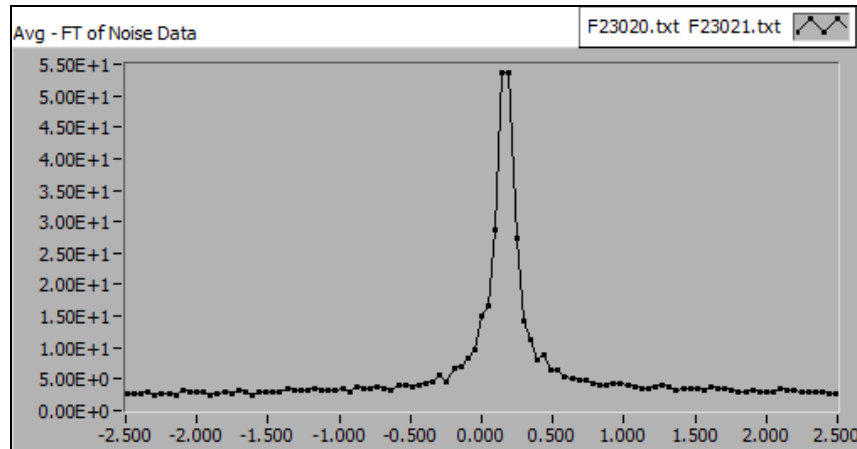


Figure 7. Average FT of 60 10-s data collections runs for the stiff cantilever. The area under the peak corresponds to $\langle x(t)^2 \rangle$ for the cantilever which sits on a noise baseline.

4. Results and Discussion—Soft Cantilever

The Cornell soft cantilevers are known to have a spring constant of ~ 0.0001 N/m. At a temperature of 4.2 K, this cantilever should have a Brownian motion value of 0.76 nm RMS. Our first measurement of the soft cantilevers at 5.2 and 22.5 K resulted in RMS values of $x(t)$ of 1.81 and 1.91 nm RMS, respectively. Thus, this cantilever also appears to be base driven.

However, before concluding that the nanopositioners vibrate too much, we decided to turn down the IF laser optical power. We had typically been operating the IF with ~ 400 nW onto the cantilever, so we turned it down to ~ 200 nW. This corrected the problem. Figure 8 shows $\langle x(t)^2 \rangle$ versus temperature for the soft cantilever. Since all the data fall on a straight line down to the lowest temperature investigated, we know the cantilever is not significantly base driven or driven by the IF optical power. When contrasting this to the data plotted in figure 5, we determined that all of $\langle x(t)^2 \rangle$ can be attributed to Brownian motion. The straight line is a fit to the data, and using the Equipartition theorem, gives a spring constant of 0.000103 N/m. We conclude that we have been using too much IF power for the soft Cornell cantilevers.

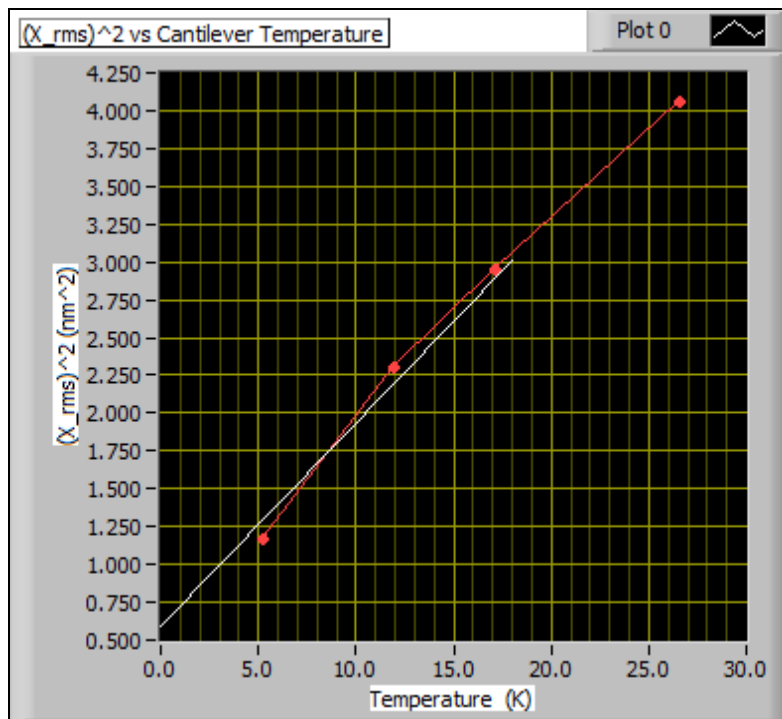


Figure 8. Soft cantilever $\langle x(t)^2 \rangle$ vs. temperature. Since the data all fall on a straight line down to the lowest temperature investigated, we know it is not significantly base driven and all of $\langle x(t)^2 \rangle$ can be attributed to Brownian motion. The straight line is a fit to the data and gives a spring constant of 0.000103 N/m.

Figure 8 was generated without performing an FT analysis of the software lock-in output. We were able to skip this step since the soft spring constant is 100 times softer than the stiff spring constant. Resulting in the soft cantilever's Brownian motion being 10 times greater than the stiff cantilever. With the greater motion, the IF noise floor becomes insignificant.

Eric Moore and John Marohn (3, 4) of Cornell University have observed that cantilevers displaying 4 K Brownian motion can have significantly higher frequency noise than would be predicted by Brownian motion alone. Therefore, since the soft cantilever achieves Brownian motion for $\langle x(t)^2 \rangle$ at the lower IF power, we performed frequency noise measurements on it to test this observation. Using the Marohn work, we extracted an effective temperature from the cantilever. From Marohn's white paper (2), we used the following equation:

$$P_{\dot{x}}^{therm}(f) = \frac{k_B T}{2\pi^2 x_{rms}^2 k \tau_0}. \quad (2)$$

The Q of the cantilever was measured at each temperature and found to decrease as the temperature rises.

Some of our initial measurements indicated temperatures as high as 120 K. The software package Extract used to analyze the data has been extensively tested and was believed to be working correctly (10). However, we decided to perform an additional independent test of its performance. Following Marohn (11), we recorded the Brownian motion history $x(t)$ of a 5.2 K undriven cantilever to a disk. Using Extract, we read $x(t)$ back into the program, added to it a pure sine wave to simulate the driven cantilever, and then had Extract analyze the data as if it had just acquired actual driven cantilever data. Extract's analysis returned an effective cantilever temperature of 4.8 K. We believe 4.8 K is close enough to 5.2 K to conclude that Extract is working correctly. The attractiveness of the approach of recording the Brownian motion to disk instead of attempting to simulate it is that it incorporates the actual damping time of the cantilever into the Brownian motion and the correct Brownian motion amplitude for the cantilever's temperature. This avoids having to determine whether or not simulated data accurately reflects the very small bandwidth that a high Q cantilever represents.

After once again verifying that Extract is working correctly, we obtained frequency noise data with effective temperatures significantly above that of the Brownian motion of the cantilever. We collected data for the driven cantilever three ways: (1) via a closed loop using the SC-Solutions frequency controller, the scFDC; (2) via an open loop, where the cantilever was driven with the Stanford Research Instruments signal generator SRS345; and (3) by turning off the amplitude drive, grounding the Attocube nanopositioner and recording the data as the cantilever rang down. Approach three allows us to measure the frequency noise of the cantilever with no drive electronics attached to it. However, attached to the top of the probe is still ~6 m of unshielded instrumentation cable that is grounded back in the instrumentation rack. This grounded-at-one-

end cable acts as a receiving antenna for environmental noise, of course. Modification of the instrumentation and further testing will be required to determine the effect of grounding the wires to the piezoelectric drive elements at the top of the probe.

Figure 9 summarizes our results. It shows the apparent temperature of the driven cantilever extracted using the Marohn approach versus the actual base temperature of the cantilever for the driven and undriven cantilever. Two points are evident from this figure: (1) our closed loop drive electronics is contributing significant frequency noise (we do not yet know if the open loop driven cantilever is significantly different from the closed loop driven cantilever) and (2) the undriven, freely ringing down cantilever appears to respond to the thermal excitation while saturating at lower base temperatures; however, the slope of the thermal response is wrong. It should be 1, while here it is somewhat over 2.

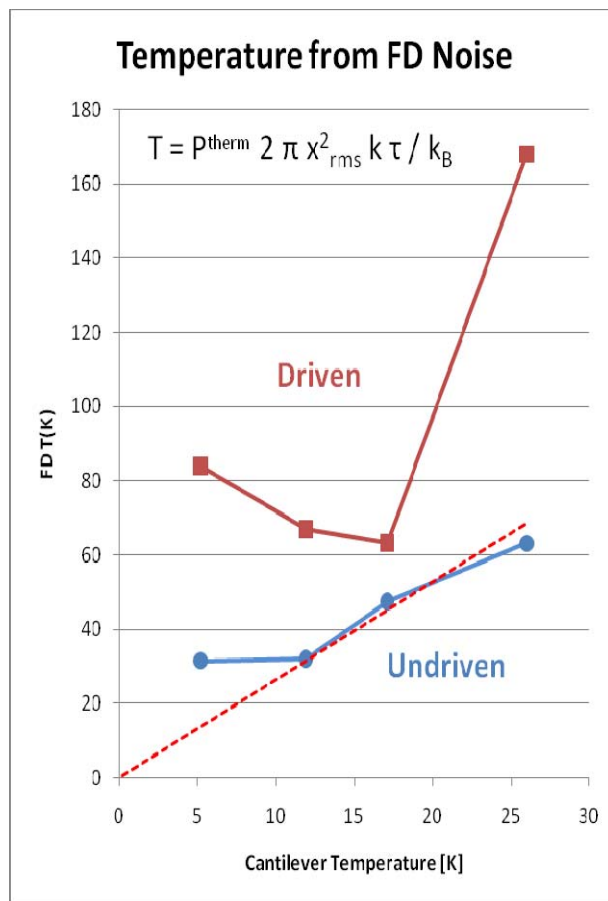


Figure 9. Soft cantilever frequency noise vs. temperature. Data plotted as squares is for a cantilever driven closed loop. The circles are the undriven cantilever measured during ring down.

It should be noted that we are aware that it is possible that we are analyzing the data for the undriven cantilever incorrectly. The apparent temperature of the cantilever derived from the frequency noise is a sensitive function of $x(t)$ because $x(t)$ appears squared in the equation for the

temperature. We use the RMS value of $x(t)$ over the entire 10 s of data collection period for x_{rms} . Since at 5.2 and 26 K, the ring down time is 16.6 and 13.0 s, respectively, there are significant changes in x_{rms} during data collection.

Perhaps this accounts for the differences between the driven and undriven cases (unlikely), or why the slope is somewhat over two instead of one (possibly). Further analysis is needed.

5. Conclusions

We learned that for the software implemented lock-in, it is important to prefilter the data with a bandpass filter with a bandwidth of 10% of f_c before multiplying it by the local oscillator. Otherwise, too much noise is introduced into the x and y values. High pass filtering at 500 Hz is not sufficient.

We concluded that we have been using too much IF power for the soft Cornell cantilevers. Attempts to turn the IF optical power down below 200 nW resulted in operating the laser too near threshold and introduced significant frequency noise. At a future time, we will introduce more attenuation after the laser diode so the laser does not have to operate near threshold and perform tests with even lower optical power.

We also determined that just because a cantilever achieves a 5 K Brownian motion does not mean its frequency noise is 5 K. We have been operating our IF system at an optical power of 400 nW, and this has been introducing over an order of magnitude more frequency noise that would be expected from Brownian motion, assuming the current cantilever is typical. This issue explains why our cantilever-enabled readout of magnetization inversion transients (CERMIT) data did not look as good as the amplitude data from years ago using SiN cantilevers with spring constants of only 0.01 N/m.

However, the failure of $\langle x(t)^2 \rangle$ to equal Brownian motion at 400 nW differs from two previous measurements of $\langle x(t)^2 \rangle$ versus T for a cantilever mounted on the probe head mechanical ground. For both of those measurements, $\langle x(t)^2 \rangle$ equaled Brownian motion. All cantilevers were Cornell soft cantilevers with spring constants of ~ 0.0001 N/m, but they were not the same cantilever. The question remains, does the current cantilever absorb more light for some reason? Further testing will have to be done to explore this.

6. References

1. Obukhov, Y.; Fong, K. C.; Daughton, D.; Hammel, P. C. Real Time Cantilever Signal Frequency Determination Using Digital Signal Processing. *J. Appl. Phys.* **2007**, *101*, 034315-1–034315-5.
2. Marohn, J. *Frequency Noise*, white paper, Cornell University, 24 February 2008.
3. Moore, E.; Marohn, J. Private communication. Cornell University, 2010.
4. Moore, E. Private communication. Cornell University, 2010.
5. Park scientific instruments, model #: MLCT-NOHW, part #: 00-103-0941, wafer #: 170-40-8.
6. Hickman, S. cantilever fabricated by, Cornell University, 2008.
7. Gmelin, E.; Asen-Palmer, M.; Reuther, M.; Villar, R. Thermal Boundary Resistance of Mechanical Contacts Between Solids at Sub-ambient Temperatures. *J. Phys D: Appl. Phys.* **1999**, *32*, R19–R43.
8. Bruland, K. J.; Garbini, J. L.; Dougherty, W. M.; Chao, S. H.; Jensen, S. E. Thermal Tuning of a Fiber-optic Interferometer for Maximum Sensitivity. *Rev. Sci. Instr.* **1999**, *70* (9), 3542–3544.
9. Marohn, J. *Harmonic Oscillator Brownian Motion*, white paper, Cornell University, 27 March 2001.
10. Smith, D. D. *Description of Software Package Extract for the Characterization of the Amplitude and Frequency Noise Properties of Cantilevers Used for Nano-MRI*; ARL-TR-4995; U.S. Army Research Laboratory: Adelphi, MD, September 2009.
11. Marohn, J. *Spin Readout and Imaging Protocol Development for Magnetic Resonance Force Microscopy of Organic Thin-Film Samples*; SBIR final report; Contract DAAD19-02-D-001, 2007.

List of Symbols, Abbreviations, and Acronyms

3-D	three-dimensional
ARL	U.S. Army Research Laboratory
ADC	analog-to-digital converter
BeCu	beryllium-copper
CERMIT	cantilever-enabled readout of magnetization inversion transients
FT	Fourier transform
He	helium
IF	interferometer
MRFM	magnetic resonance force microscopy
MRI	magnetic resonance imaging
PSD	power spectral density
RF	radio frequency
RMS	root mean square
Si	silicon
SiN	silicon nitride
SNR	signal-to-noise ratio

1 DEFENSE TECHNICAL
(PDF INFORMATION CTR
only) DTIC OCA
8725 JOHN J KINGMAN RD
STE 0944
FORT BELVOIR VA 22060-6218

1 HC DIRECTOR
US ARMY RESEARCH LAB
IMNE ALC HRR
2800 POWDER MILL RD
ADELPHI MD 20783-1197

1 HC DIRECTOR
US ARMY RESEARCH LAB
RDRL CIM L
2800 POWDER MILL RD
ADELPHI MD 20783-1197

1 HC DIRECTOR
US ARMY RESEARCH LAB
RDRL CIM P
2800 POWDER MILL RD
ADELPHI MD 20783-1197

10 HCS DIRECTOR
US ARMY RESEARCH LAB
RDRL SEE O DORAN SMITH
2800 POWDER MILL RD
ADELPHI MD 20783-1197

5 HCS CORNELL UNIVERISTY
DEPT OF CHEMISTRY & CHEMICAL BIOLOGY
DR JOHN MAROHN
150 BAKER LABORATORY
ITHACA NY 14853-1301

ABERDEEN PROVING GROUND

1 HC DIR USARL
RDRL CIM G (BLDG 4600)